

# Study of low energy $\text{Si}_5^-$ and $\text{Cs}^-$ implantation induced amorphisation effects in Si(100)

H. P. Lenka,<sup>1</sup> B. Joseph,<sup>1,\*</sup> P. K. Kuri,<sup>1</sup> G. Sahu,<sup>1</sup> P. Mishra,<sup>2</sup> D. Ghose,<sup>2</sup> and D. P. Mahapatra<sup>1,†</sup>

<sup>1</sup> *Institute of Physics, Sachivalaya Marg, Bhubaneswar - 751005, India*

<sup>2</sup> *Saha Institute of Nuclear Physics, 1/AF Bidhan Nagar, Kolkata - 700064*

(Dated: October 8, 2018)

The damage growth and surface modifications in Si(100), induced by 25 keV  $\text{Si}_5^-$  cluster ions, as a function of fluence,  $\phi$ , has been studied using atomic force microscopy (AFM) and channeling Rutherford backscattering spectrometry (CRBS). CRBS results indicate a nonlinear growth in damage from which it has been possible to get a threshold fluence,  $\phi_0$ , for amorphisation as  $2.5 \times 10^{13}$  ions  $\text{cm}^{-2}$ . For  $\phi$  below  $\phi_0$ , a growth in damage as well as surface roughness has been observed. At a  $\phi$  of  $1 \times 10^{14}$  ions  $\text{cm}^{-2}$ , damage saturation coupled with a much reduced surface roughness has been found. In this case a power spectrum analysis of AFM data showed a significant drop, in spectral density, as compared to the same obtained for a fluence,  $\phi < \phi_0$ . This drop, together with damage saturation, can be correlated with a transition to a stress relaxed amorphous phase. Irradiation with similar mass  $\text{Cs}^-$  ions, at the same energy and fluence, has been found to result in a reduced accumulation of defects in the near surface region leading to reduced surface features.

## I. INTRODUCTION

Cluster ion implantation can be regarded as a fore-runner technology as compared to the conventional ion implantation technique used to dope sub-micron devices [1, 2]. Using cluster ions very shallow implantation can be achieved at very low energy. However, with cluster implantation, nonlinear effects arising in the energy loss processes, as a result of the correlated motion of the constituent atoms, play an important role in deciding the defect structure near the target surface. In addition to resulting in a nonlinear growth in subsurface damage, cluster ion impact, through sputtering, can also result in kinetic roughening and smoothening of the surface exposed [3]. In view of all this, there has been a lot of activities involving low energy cluster ion irradiation related to nonlinear sputtering [4], nonlinear damage and defect production [5, 6, 7], along with the formation of various kind of surface features [8, 9, 10, 11, 12].

In connection with the above, Si, presents itself as a very important material where low energy cluster ions can be used for shallow implantation, of interest to technology. In some earlier work, contrary to common expectation, amorphisation upon ion irradiation has been shown to start from the surface rather than the ion projected range [13]. Results of Molecular dynamics (MD) simulations with 5 keV Si, show that the ion impacts produce unrelaxed amorphous patches that have a fast quenched, liquid like structure [14]. With increase in ion fluence these regions overlap producing a continuous amorphous layer [15]. In fact, with increase in ion fluence, there is a superlinear growth of amorphous volume fraction with a lot of stress build up in the matrix. At

high fluence there is an abrupt transition to a state with a flat amorphous-to-crystalline (a/c) interface [16, 17]. In such a case, out of plane plastic flow with a reduction in the in-plane stress have been observed [18]. All this suggest that ion irradiation induced amorphisation in Si is more like a *phase transition*, initiated by a spontaneous collapse of the damaged region. Very recent MD simulations carried out by Marqués *et al* show it to be initiated by a high concentration of *interstitial-vacancy (IV) pairs* or *bond defects*, formed in the system [19]. Similar results have also been shown by Nord *et al* [20] who have pointed out that the subsequent transition resulting in a uniform amorphous layer is neither a complete homogeneous nor a complete heterogeneous mechanism. This makes Si an ideal system to study using low energy cluster ions where such a transition to a complete amorphous state is expected at a lower fluence, primarily because of overlapping of collision cascades coming from constituent atoms.

In the present paper we show some results of a systematic study of the subsurface damage produced and the surface features generated in Si(100), from  $\text{Si}_5^-$  and a similar mass  $\text{Cs}^-$  ion implantation at 25 keV. Channeling Rutherford backscattering spectrometry (CRBS) and Atomic force microscopy (AFM) have been used for sample characterization. Increase in cluster ion fluence has been found to result in a nonlinear growth and saturation in damage leading to amorphisation. The transition to an amorphised state is found to be associated with a significant drop in the power spectral density of AFM data which initially increases with increase in fluence.

## II. EXPERIMENT

Cleaned Si(100) wafers (*p*-type, 1-2.5  $\Omega\text{cm}$ ) were irradiated with 25 keV singly charged negative ions *viz*  $\text{Si}_5^-$  and  $\text{Cs}^-$  from a SNICS-II ion source (NEC, USA) using a low energy ion implanter facility. Mass analysis of the cluster ions was carried out using a 45° sector

---

\*Present address: Istituto Tecnologie Avanzate, Contrada Milo 91100, Trapani, Italy

†Author to whom any correspondence should be addressed; electronic mail: dpm@iopb.res.in

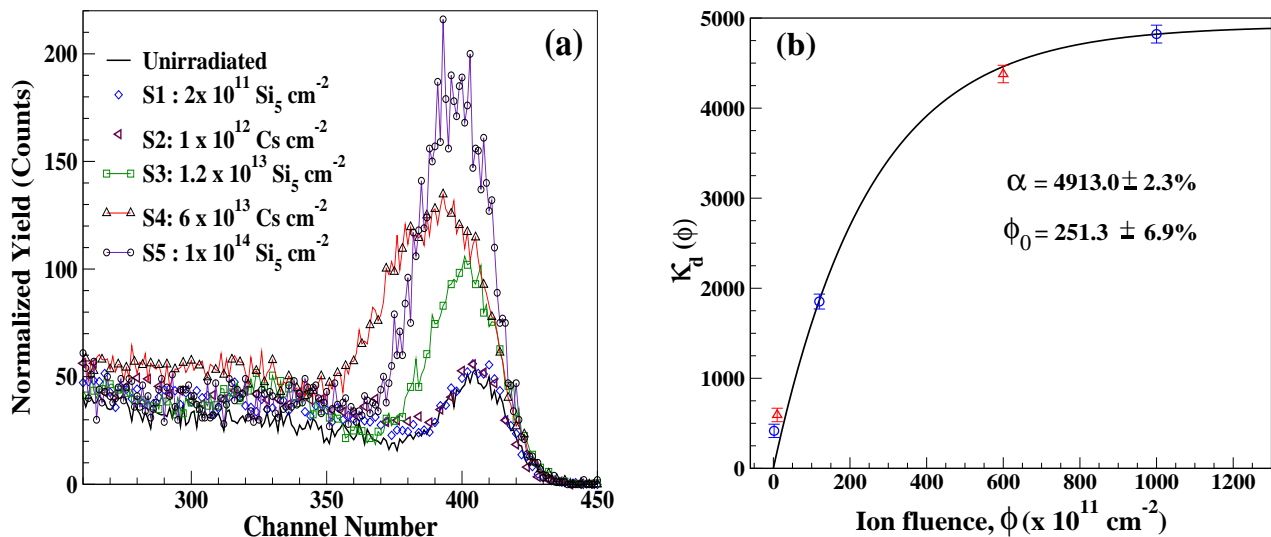


FIG. 1: (Color online) (a) CRBS spectra for Si(100), implanted with 25 keV  $\text{Si}_5^-$  and  $\text{Cs}^-$  for different values of implantation fluence together with the same for a virgin sample. (b) Fluence ( $\phi$ ) dependence of displaced Si atoms,  $\kappa_d(\phi)$ , for various implantations. Circles and triangles represent data for  $\text{Si}_5^-$  and  $\text{Cs}^-$  implantations respectively. The continuous curve is a fit to the data points with clusters.

magnet ( $\text{ME}/q^2 = 18 \text{ MeV amu}$ ). The base pressure in the target chamber during irradiations was maintained around  $2 \times 10^{-7}$  mbar. All the irradiations were carried out at room temperature with a beam flux of  $2\text{-}3 \times 10^{10}$  ions  $\text{cm}^{-2}\text{sec}^{-1}$  (ion current of  $2 - 3 \text{ nA}$ ) at  $\sim 7^\circ$  off the sample normal. In each case one part of the sample was kept unimplanted to serve as a reference. Five samples named S1-S5 were systematically irradiated with ions of similar mass ( $\text{Si}_5^-$  or  $\text{Cs}^-$ ) with gradually increasing ion fluence from  $2 \times 10^{11} \text{ cm}^{-2}$  to  $1 \times 10^{14} \text{ cm}^{-2}$ . Three of these, *viz* S1, S3 and S5 were irradiated using  $\text{Si}_5^-$  clusters to fluences of  $2 \times 10^{11} \text{ cm}^{-2}$ ,  $1.2 \times 10^{13} \text{ cm}^{-2}$  and  $1 \times 10^{14} \text{ cm}^{-2}$  respectively. The remaining two samples, S2 and S4 were irradiated with 25 keV  $\text{Cs}^-$  ions to fluences of  $1 \times 10^{12} \text{ cm}^{-2}$  and  $6 \times 10^{13} \text{ cm}^{-2}$  respectively. These data are shown in Table. 1.

TABLE I: Sample names, ions used and integrated fluence.

Samples	fluence	Ion species of 25 keV total energy
S1	$2 \times 10^{11} \text{ cm}^{-2}$	$\text{Si}_5^-$
S2	$1 \times 10^{12} \text{ cm}^{-2}$	$\text{Cs}^-$
S3	$1.2 \times 10^{13} \text{ cm}^{-2}$	$\text{Si}_5^-$
S4	$6 \times 10^{13} \text{ cm}^{-2}$	$\text{Cs}^-$
S5	$1 \times 10^{14} \text{ cm}^{-2}$	$\text{Si}_5^-$

CRBS measurements were carried out on all the samples with 1.35 MeV  $\text{He}^+$  with a Si surface barrier detector placed at  $130^\circ$  relative to the incident beam direction. The measurements were carried out at a steady beam current of  $5 \text{ nA}$ , using the 3 MV Pelletron accelerator (9SDH2, NEC, USA) facility at IOP, Bhubaneswar. In case of unirradiated Si(100), the reduction in the inte-

grated total yield from random to a channeled spectrum was found to be  $\sim 5\%$ .

Following irradiation, the surface topography was examined by AFM in the tapping mode, using a multi-mode scanning probe microscope (Nanoscope IV, Veeco, USA). Measurements were performed in ambient condition using a Si cantilever with a nominal tip radius less than  $\sim 10 \text{ nm}$ . Image processing and analysis of the AFM data were carried out using the standard WSxM software package [21, 22].

### III. RESULTS AND DISCUSSION

The CRBS results as measured for all the five samples *viz.* S1-S5 and a virgin sample (unirradiated area), are presented in Fig. 1(a). From the figure, one can observe a gradual increase in surface peak intensity with increase in ion fluence,  $\phi$ . This increase in the area of the surface peak, over and above that in the virgin sample, indicates growth in damage produced with increase in the number of displacements. In line with this, the lowest fluence irradiation is found to induce very little damage, too small to be seen through CRBS data. However, increase in irradiation fluence from S1 to S3 (with cluster ions) and that for S2 to S4 (for Cs ions) are seen to result in enhancements of the surface peak, indicating an increase in defect production near the surface. For the sample S5, with the highest cluster irradiation fluence, the surface peak is seen to be the most intense. This sample, with a total single atom fluence of  $5 \times 10^{14} \text{ cm}^{-2}$  is expected to have an amorphous layer with a thickness of  $\sim 8 \text{ nm}$  extending from the surface [23].  $\text{Cs}^-$  irradiation to a

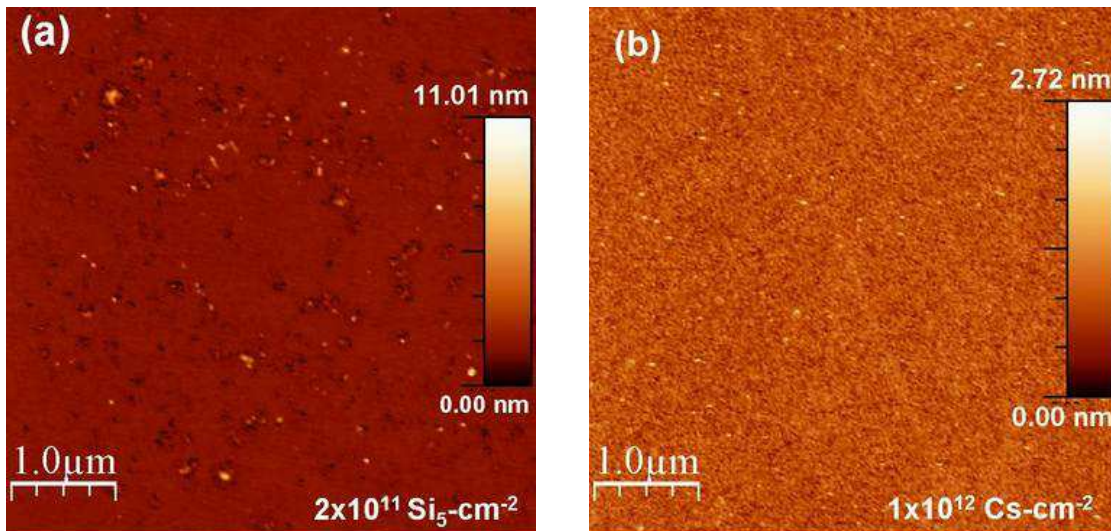


FIG. 2: (Color online) Surface morphology of samples (a) S1 and (b) S2. Both samples have the same monomer fluence as that of S2, *i.e.*  $1 \times 10^{12}$  atoms  $\text{cm}^{-2}$ .

fluence, 0.6 times as that of S5, is seen to produced a damage distribution going deeper into the bulk.

Now we look at the difference in the surface peak areas between the irradiated and the unirradiated regions, which at lower irradiation fluence, is proportional to the number of displaced Si atoms, in the irradiated lattice. We denote this as  $\kappa_d$  which has been estimated for various samples integrating data (fig 1 (a)) between channels 340 and 440. Fig. 1(b) shows ion fluence,  $\phi$ , dependence of  $\kappa_d$  for various implantation fluence. From the figure, one can see a clear nonlinear growth and saturation in damage with increase in ion fluence. Similar results, regarding a nonlinear growth in damage production and saturation has been seen earlier in case of 5 keV/atom  $C_n$  cluster irradiations of Si(100) [6].

To get an idea about damage saturation and the amorphisation threshold, as has been done earlier [6, 24], we have fitted the three points as obtained for  $Si_5$  irradiation to an equation of the form,

$$\kappa_d(\phi) = \alpha(1 - e^{-\phi/\phi_0}) \quad (1)$$

where  $\alpha$  is a constant and  $\phi_0$  corresponds to the threshold fluence for damage saturation. The best fit, as indicated by the smooth curve in Fig. 1(b), yields a value of  $\phi_0$  equal to  $(2.5 \pm 7\%) \times 10^{13}$   $\text{cm}^{-2}$ . One can see, at a fluence of  $6 \times 10^{13}$   $\text{cm}^{-2}$ , the  $\kappa_d$  value corresponding to 25 keV Cs atoms is almost the same as that expected for a similar mass  $Si_5$  cluster at the same energy. This means, the heavy single atom induced cascades produce almost the same amount of damage or defects as those generated by a similar mass cluster ion. At this high fluence, because of overlapping of damage produced cluster induced nonlinear effects are difficult to be detected. However, in this case there are defects extending into the bulk while

those for a cluster ion are better confined in a surface layer.

The above  $\phi_0$  value of  $2.5 \times 10^{13}$   $\text{cm}^{-2}$  as obtained for  $Si_5$  clusters, where damage saturation starts, corresponds to a total atomic fluence of  $\sim 1.25 \times 10^{14}$   $\text{cm}^{-2}$ . This agrees with the finding of Agarwal *et al.* [23] who have shown the amorphisation threshold, for 5 keV Si in Si, to be  $1 - 3 \times 10^{14}$   $\text{cm}^{-2}$ . In fact, with clusters, as expected the present value agrees with the lower limit. In view of this, at an  $Si_5$  cluster fluence of  $1 \times 10^{14}$   $\text{cm}^{-2}$  (corresponding to an atomic fluence of  $5 \times 10^{14}$   $\text{cm}^{-2}$ ), we are already well above the threshold for amorphisation.

#### A. Surface features and AFM data

As has been mentioned earlier, AFM has been used to study the surface topography in various samples. Some AFM pictures (top view), for  $(5 \mu\text{m} \times 5 \mu\text{m})$  scanned areas, taken on the samples are shown in Figs. 2 and 3. Figs 2(a) and (b) correspond to samples S1 and S2, while Figs. 3(a) and (b) correspond to samples S3 and S4 respectively.

Usually the features on irradiated surfaces are described through a height-height correlation function which contains three important roughness parameters: (i) the vertical correlation length  $\sigma$ , (ii) the lateral correlation length  $\xi$  and (iii) the roughness exponent  $\alpha$  [25, 26, 27, 28]. The lateral correlation length,  $\xi$ , describes the lateral characteristics of the surface, the roughness exponent  $\alpha$  describing the static scaling properties. The most commonly reported parameter of surface roughness *i.e.*  $\sigma$ , or the root-mean-square (rms) roughness, characterizes the surface, only along the vertical direction. This is defined as standard deviation of

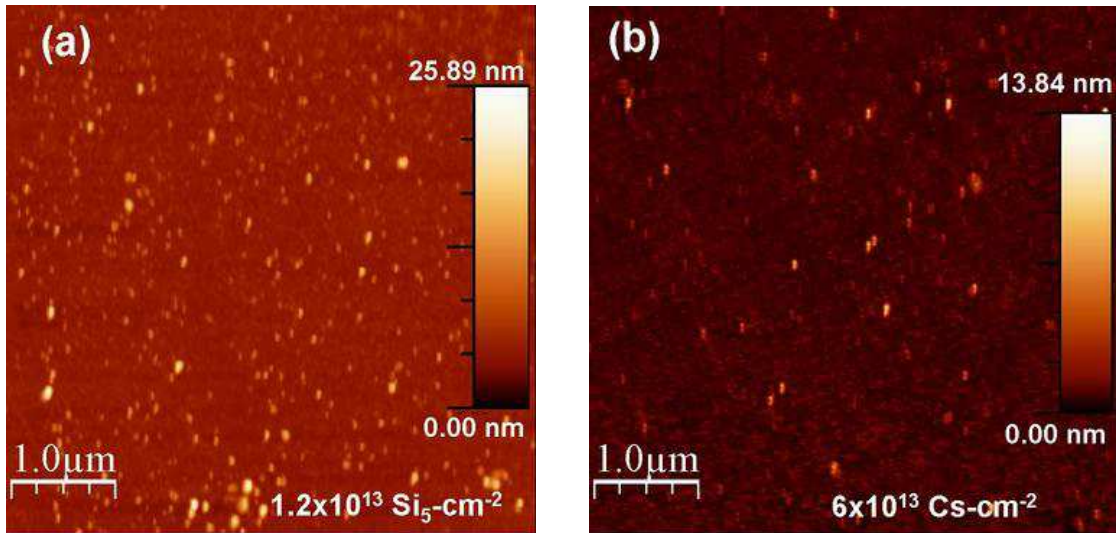


FIG. 3: (Color online) Surface morphology of samples (a) S3 and (b) S4. Both samples have the same monomer fluence as that of S3, *i.e.*  $6 \times 10^{13}$  atoms  $\text{cm}^{-2}$ .

the surface height profile,  $h(x, y)$ , at each point  $(x, y)$  of a reference surface plane from the mean height  $\langle h \rangle$ , as given by,

$$\sigma = \left[ \frac{1}{N} \sum_{i=1}^N (h_i - \langle h \rangle)^2 \right]^{1/2} \quad (2)$$

where  $N$  is the number of pixels,  $h_i = h(x, y)$  being the height at the  $i^{\text{th}}$  pixel.

In case of the sample S1, as shown in Fig 2(a), one can clearly see black dots corresponding to nanometer sized pits and bright spots corresponding to hillocks (color bars indicating the heights). The observed hillocks are seen to have heights ranging between 1 – 6  $\text{nm}$  with average height of 1.64 $\text{nm}$ . It has an rms roughness,  $\sigma$  of 0.34  $\text{nm}$ . Compared to this, there was hardly any surface feature in the case of a pristine Si(100) sample (AFM data not shown here). The rms roughness,  $\sigma$ , of the pristine sample, was found to be 0.13  $\text{nm}$ , which is about one third of that for S1, corresponding to a smooth polished surface.

In case of the lowest fluence Cs implanted sample, S2, the  $\sigma$  for surface roughness was found to be 0.21  $\text{nm}$ , lying between that for S1 (0.34 $\text{nm}$ ) and the pristine sample (0.13 $\text{nm}$ ). What is important to see here is that Cs implantation to a five times higher fluence is not able to generate a surface roughness as observed in case of S1. Compared to the above, S3, implanted with Si<sub>5</sub> clusters, to a fluence sixty times that of the sample S1, was found to have an rms roughness,  $\sigma$ , of 1.21  $\text{nm}$ . However, the above sixty-fold increase in Si<sub>5</sub> cluster fluence from S1 to S3, did not result in a proportionate increase in the number of nanohillocks in S3. The surface topography of the sample S4, implanted with Cs to a fluence five

times that of S3 is shown in Fig. 3(b). However, a much smaller number of nanohillocks, compared to the S3 sample, could be seen. It has a  $\sigma$  value of 0.42 $\text{nm}$  which is significantly smaller than that observed for S3. The enhanced surface roughness as seen with Si<sub>5</sub> implantations in S1 as compared to S2 (and S3 as compared to S4), even with lower fluence of irradiations, are primarily due to molecular effects coming from overlapping of collision cascades of constituent atoms. Such effects are absent during a single mass Cs irradiation which results in lower damage accumulation and lower surface roughness. Compared to all the above, the  $\sigma$  value of surface roughness observed for the sample S5, which had the highest cluster ion fluence, turned out to be 0.21 $\text{nm}$ . This was quite small compared to the same obtained for S3, irradiated with an almost one order of magnitude lower fluence.

However, the parameter  $\sigma$  is not enough to give a full characterization of the surface because it is limited by its sensitivity only in the vertical direction. For example, two images with exactly the same rms roughness values can have different surface morphologies [29]. In view of this, a power spectral density (PSD) analysis is often used to look at surface features and their possible origin [30, 31, 32, 33]. The PSD analysis is accomplished by radially averaging the square magnitude of the coefficients of the two-dimensional Fourier Transform of the digitized surface profile  $h(x, y)$  defined by

$$C(q) = \frac{1}{L^2} \left| \iint \frac{d^2r}{2\pi} \exp^{-iq \cdot r} \langle h(r) \rangle \right|^2 \quad (3)$$

where  $h(r) = h(x, y)$ . Here  $q$  is the spatial frequency in reciprocal space,  $L^2$  is the scanned area of length  $L$  and  $h(r)$  is the height at the position  $r$ . The PSD, which is the Fourier transform of the height-height correlation

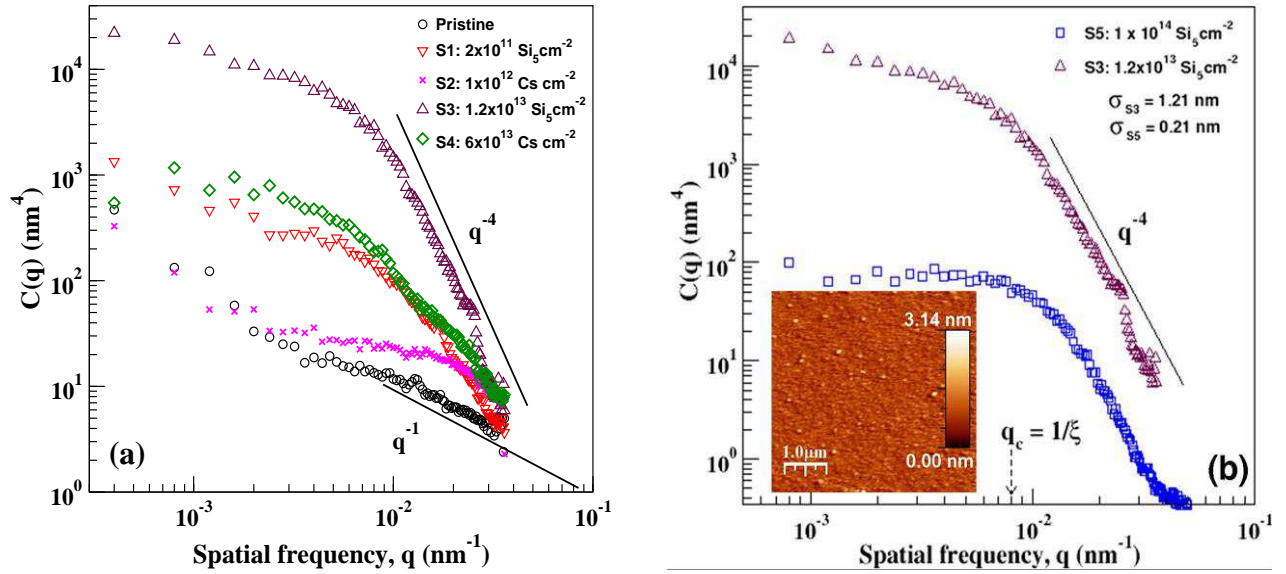


FIG. 4: (Color online) (a)  $C(q)$ , as a function of spatial frequency  $q$ , for Si<sub>5</sub> and Cs irradiated Si(100) at different irradiation fluence. ○, un-irradiated Si; ▽, S1 (with Si<sub>5</sub> at  $2 \times 10^{11} \text{ cm}^{-2}$ ); □, S2 (with Cs monomer fluence  $1 \times 10^{12} \text{ cm}^{-2}$ ); △ S3 (with Si<sub>5</sub> at  $1.2 \times 10^{13} \text{ cm}^{-2}$ ); ◇, S4 (with Cs at  $6 \times 10^{13} \text{ cm}^{-2}$ ). (b)  $C(q)$  for samples S3 and S5. Inset shows the AFM image for S5 for a scan size of  $5 \mu\text{m} \times 5 \mu\text{m}$ .

function, thus turns out to be a function of only one parameter, spatial frequency,  $q$ . Identification of various processes for surface transport [34] is carried out using the stochastic rate equations for the surface evolution [35]. In this analysis [36],  $C(q) = 2D(q)/[\Sigma a_\gamma q^\gamma]$ , where  $D(q)$  is a term coming from noise correlation,  $a_\gamma$  being expansion coefficients. The index  $\gamma$  has values of 1, 2, 3 and 4 representing four modes of surface transport *viz.* viscous flow, evaporation-condensation, volume diffusion and surface diffusion respectively. This index is further related to the roughness scaling exponent,  $\alpha$  through the relation  $\gamma = 2(\alpha + 1)$ .

The PSD spectra,  $C(q)$ , for all the samples S1 to S4 and pristine, are shown in Fig. 4(a). One can see, there is an increase in spectral strength in the order pristine, S2, S1, S4 and S3 where the pristine has the lowest and S3 has the highest values. This order is exactly the same if one orders the samples according to the  $\sigma$  values for the surface roughness. S2 and S4 have five times higher ion fluence as compared to S1 and S3 respectively. But the surface features produced are seen to be much reduced.

Having seen the above general features we now try to look at other details of  $C(q)$ . One can see that the pristine sample ( $\sigma = 0.13 \text{ nm}$ ) has a cut off value,  $q_c$ , which is about  $0.001 \text{ nm}^{-1}$ . This corresponds to a large correlation length,  $\xi$  of  $1 \mu\text{m}$ . Further, it has a  $\gamma$  close to 1. The Cs implanted sample, S2, has also a smooth surface ( $\sigma = 0.21 \text{ nm}$ ). The corresponding  $C(q)$  indicates surface modulations over a similar length scale as the pristine sample. Compared to this, the Si<sub>5</sub> cluster implanted S1 sample, with one fifth of the fluence as in S2,

shows modulations with a higher value of  $q_c$  of the order of  $0.006 \text{ nm}^{-1}$ . This indicates a correlation length,  $\xi$ , of the order of  $170 \text{ nm}$ . As shown earlier, it has a  $\sigma$  value of  $0.34 \text{ nm}$ . The Fourier index  $\gamma$  is seen to be about 2.5. This yields an  $\alpha$  value of 0.25, indicating the surface to be self affine with anisotropic scaling along lateral and perpendicular directions.

The  $C(q)$  for the higher fluence Cs irradiated sample, S4, shows a  $q_c$  which is almost similar to that for the lower fluence Si<sub>5</sub> implanted sample, S1, indicating a similar correlation length,  $\xi$ , of  $170 \text{ nm}$ . However, it shows a  $\gamma$  value of around 2.2 resulting in an  $\alpha$  value  $\sim 0.1$ . With a  $\sigma$  value of  $0.42 \text{ nm}$ , it has a higher roughness. This means, with a 300 times higher fluence, Cs ions generate similar surface features as obtained for a low dose Si<sub>5</sub> implanted sample, S1. Compared to this, the Si<sub>5</sub> cluster implanted sample S3, with a fluence which is one fifth of that in S4, shows a  $\gamma$  value close to 4, indicating an  $\alpha$  value close to unity. This indicates the surface modulations to be self similar. But this sample has the highest surface roughness,  $\sigma$  of  $1.21 \text{ nm}$  with an average height of  $5 \text{ nm}$ .

Now we look at what happens when cluster fluence is increased to a value well beyond the amorphisation threshold as in case of S5. An AFM image of the top view of S5, taken with a ( $5 \mu\text{m} \times 5 \mu\text{m}$ ) scan size is shown in Fig. 4(b). The  $C(q)$  spectrum for S5 is also shown along with that for S3 in the same figure. One can clearly see that increasing the cluster ion fluence from  $1.2 \times 10^{13}$  to  $1 \times 10^{14} \text{ cm}^{-2}$ , in going from S3 to S5, has resulted in no further change in the  $\gamma$  value which has been found to saturate at 4. But the surface modulations changed to have a  $\sigma$  value of  $0.21 \text{ nm}$  with a correlation length

$\xi \sim 125nm$ . With an  $\alpha$  value close to 1, the surface features in S5 are self similar indicating isotropic scaling. However, as compared to the S3 case,  $C(q)$  shows a significant reduction in the magnitude. At  $q_c$ , the ratio between the two is about 33. This can also be seen using the formula  $C(q) = [\alpha\sigma^2\xi^2/\pi]$  at  $q_c = 1/\xi$ . Since S3 and S5 have almost same  $\alpha$  as well as  $\xi$  values, the ratio of the  $C(q)$ s turn out to be nearly the same as the ratio of the  $\sigma^2$  for the two cases. This is seen to be  $(1.21/0.21)^2$  which is just about right. It is important to mention that the surface modulations in S5 show a mean height of  $0.6nm$ . The small value of  $C(q)$  for S5, is therefore seen to be coming from a correlation between small but nearly equal heights with a small  $\sigma$  value. Compared to this  $C(q)$  in S3 comes from a correlation between higher heights, with an average value of  $5nm$ , again with a much higher value of  $\sigma$ .

Earlier, 5 keV Si impact on Si has been shown to result in creation of amorphous pockets coming from local melting and rapid quenching [14]. The stress produced can result in formation of pits and bumps on the surface. This is in addition to roughening resulting from sputtering. This local melting and the associated movement of atoms, at lower fluence as in S1, may be responsible for a  $\gamma$  value between 2 and 3. It also leads to a higher surface roughness as compared to a pristine sample. At lower fluence there are sparsely distributed amorphous pockets in the matrix. Increase in the implantation fluence results in a fast growth in the number of amorphous patches resulting in a growth in surface roughness,  $\sigma$ . This also results in a growth in mean height,  $\langle h \rangle$ , of surface structures produced, resulting in a growth of height-height correlation. Merging of amorphised regions at higher fluence, results in a building up of stress from a large number of *bond defects*. Finally there could be stress relaxation as the damaged lattice becomes unstable. This could result in a transition to a state with smaller surface features which is achieved by an effective movement of atoms in a lateral direction. This could be the reason behind getting a  $\gamma$  value close to 4 as proposed for surface diffusion. This is probably how a smooth amorphous to crystalline interface can occur in Si under high fluence ion irradiation [16, 17]. This way crystalline to amorphous transition in Si, upon ion irradiation, is more like a phase transition induced by an accumulation of sufficient number of defects which was also suggested by several groups earlier

[16, 37, 38]. In the present case, onset of this occurs at a cluster fluence of around  $2.5 \times 10^{13} \text{ cm}^{-2}$ . For a much higher cluster fluence (as in S5), a continuous amorphous layer parallel to the surface is produced, leading to much reduced values for  $\sigma$  and  $C(q)$ . It is therefore not surprising that the  $\xi$ ,  $\alpha$  and  $\gamma$  values as obtained for S5 are very similar to those obtained for a-Si films [26]. This also confirms that the top surface of the S5 sample is actually amorphised, in agreement with channeling data (Fig. 1(b)) where saturation in damage production has been obtained. It is also important to realize that  $\kappa_d$  for S4 is much higher than that in case of S3 (Fig. 1(b)). In fact it is closer to that in S5. However, complete amorphisation does not occur here because the defects produced by Cs implantation are distributed over a greater depth resulting in comparatively less defect accumulation near the surface.

#### IV. CONCLUSION

To conclude, we have carried out a systematic study of 25 keV  $\text{Si}_5^-$  implantation induced damage and surface modifications in Si(100) where a nonlinear growth in sub-surface damage, with fluence, is observed. The damage produced by similar mass  $\text{Cs}^-$  ions, of the same energy, is seen to be distributed over a greater depth leading to much reduced surface features. With  $\text{Si}_5$  clusters, the threshold fluence for amorphisation of Si surface is found to be  $2.5 \times 10^{13} \text{ clusters cm}^{-2}$ , in agreement with earlier published data. Most importantly, at higher cluster fluence a transition to an amorphous state resulting in a much reduced surface roughness is indicated.

#### V. ACKNOWLEDGMENTS

The authors would like to thank A.K. Behera for the efficient running of the implanter facility and all the operators of accelerator laboratory, IOP for help during CRBS runs. The technical help regarding some preliminary AFM measurements and checks by S. Varma of IOP and S. Bhattacharjee of IMMT, Bhubaneswar are also gratefully acknowledged.

---

[1] V. N. Popok and E. E. B. Campbell, Rev. Adv. Mater. Sci. **11**, 19 (2006).  
 [2] I. Yamada, J. Matsuo, N. Toyoda, and A. Kirkpatrick, Mater. Sci. Eng. R: Reports, **34**, 231 (2001).  
 [3] Y. Teranishi, K. Kondou, Y. Fujiwara, H. Nonaka, M. Tomita, K. Yamamoto, T. Fujimoto, and S. Ichimura, Jpn. J. Appl. Phys. **45**, 5528 (2006).  
 [4] H. H. Andersen, A. Brunelle, S. Della-Negra, J. Depauw, D. Jacquet, Y. Le Beyec, J. Chaumont, and H. Bernas,

Phys. Rev. Lett. **80**, 5433 (1998); A. V. Samartsev, A. Duvenbeck, and A. Wucher, Phys. Rev. B **72**, 115417 (2005).  
 [5] L. Shao, M. Nastasi, X. Wang, J. Liu, and Wei-Kan Chu, Nucl. Instrum. Methods Phys. Res. B **242**, 503 (2006); J. Liu, X. Wang, L. Shao, X. Lu, and W. K. Chu Nucl. Instrum. Methods Phys. Res. B **190**, 787 (2002).  
 [6] H. P. Lenka, B. Joseph, P. K. Kuiry, G. Sahu, and D. P. Mahapatra, Nucl. Instrum. Methods Phys. Res. B **256**,

- 665 (2007).
- [7] A. I. Titov, A. Yu. Azarov, L. M. Nikulina, and S. O. Kucheyev Phys. Rev. B **73**, 064111 (2006).
- [8] S. Prasalovich, V. N. Popok, P. Persson, and E. E. B. Campbell, Eur. Phys. J. D **36**, 79 (2005).
- [9] J. Samela, K. Nordlund, V. N. Popok, and E. E. B. Campbell, Phys. Rev. B **77**, 075309 (2008).
- [10] H. S. Park, H. J. Jung, and W. K. Choi, Thin Solid Films **475** 36 (2005).
- [11] L. P. Allen, D. B. Fenner, C. Santeufemio, W. Brooks, and I. Yamada, J. Appl. Phys. **92**, 3671 (2002).
- [12] V. N. Popok, S. V. Prasalovich, and E. E. B. Campbell, Nucl. Instrum. Methods Phys. Res. B **207**, 145 (2003).
- [13] K. Nakajima, H. Toyofuku, and K. Kimura, Jpn. J. Appl. Phys. **40**, 2119 (2001).
- [14] T. Diaz dela Rubia and G.H. Gilmer, Phys. Rev. Lett. **74**(13), 2507 (1995).
- [15] S.U. Campisano, S. Coffa, V. Raineri, F. Priolo, and E. Rimini, Nucl. Instrum. Methods Phys. Res. B **80/81**, 514 (1993).
- [16] O.W. Holland, S.J. Pennycook, and G.L. Albert, Appl. Phys. Lett. **55**, 2503 (1989).
- [17] G. Bai and M.A. Nicolet, J. Appl. Phys. **70**, 649 (1991).
- [18] C. A. Volkert, J. Appl. Phys. **70**, 3521 (1991).
- [19] L. A. Marqués, L. Pelaz, P. López, I. Santos, and M. Aboy, Phys. Rev. B **76** 153201 (2007); L.A. Marqués, L. Pelaz, M. Aboy, L. Enríquez, and J. Barbolla, Phys. Rev. Lett. **91**, 135504 (2003); L.A. Marqués, L. Pelaz, J. Hernández, J. Barbolla, and G.H. Gilmer Phys. Rev. B **64**, 045214 (2001).
- [20] J. Nord, K. Nordlund and J. Keinonen, Phys. Rev. B **65**, 165329 (2002).
- [21] WSxM free software. Available at [www.nanotech.edu](http://www.nanotech.edu)
- [22] I. Horcas, R. Fernandez, J.M. Gomez-Rodriguez, J. Colchero, J. Gomez-Herrero, and A. M. Baro, Rev. Sci. Instrum. **78**, 013705 (2007).
- [23] A. Agarwal, T. E. Haynes, D. J. Eaglesham, H.J. Gossman, D.C. Jacobson, J. M. Poate, and Y. E. Erokhin, Appl. Phys. Lett. **70**, 3332 (1997).
- [24] M. Dobeli, R.M. Ender, U.S. Fischer, M. Suter, H.A. Synal, and D. Vetterli Nucl. Instrum. Methods Phys. Res. B **94**, 388 (1994).
- [25] E.A. Eklund, E.J. Synder, and R.S. Williams, **β285**, 157 (1993).
- [26] K.R. Bray and G.N. Parsons, Phys. Rev. B **65** 035311 (2001).
- [27] D.B. Fenner, J. Appl. Phys. **95**, 5408 (2004).
- [28] S.J. Fang, S. Haplepete, W. Chen, C.R. Helms, and H. Edwards, J. Appl. Phys. **82**, 5891 (1997).
- [29] S.J. Fang, W. Chen, T. Yamanaka, and C.R. Heims, Appl. Phys. Lett. **68**, 2837 (1996).
- [30] R. Petri, P. Brault, O. Vatel, D. Henry, E. Andre, P. Dumas, and F. Salvan, J. Appl. Phys. **75**, 7498 (1994).
- [31] W.M. Tong, R.S. Williams, A. Yanase, Y. Segawa, and M.S. Anderson, Phys. Rev. Lett. **72**, 3374 (1992).
- [32] C. Ruppe and A. Duparre; Thin Solid Films **288**, 8 (1996).
- [33] M. Senthilkumar, N.K. Sahoo, S. Thakur, and R.B. Tokas, Appl. Surf. Sci. **252**, 1608 (2005).
- [34] C. Herring, J. Appl. Phys. **70**, 3521 (1950).
- [35] W.M. Tong, E.J. Synder, R.S. Williams, A. Yanase, Y. Segawa, and M.S. Anderson, **β277**, L63 (1992).
- [36] S.G. Mayr and R.S. Averback Phys. Rev. Lett. **87**, 196106 (2001).
- [37] M.L. Swanson, J. R. Parsons and C.W. Hoelke, Radiat. Eff. **9**,249 (1971).
- [38] T. Motooka, S. Harada, and M. Ishimaru, Phys. Rev. Lett. **78**, 2980 (1997).